

GIFT: Generative Interpretable Fine-Tuning Transformers

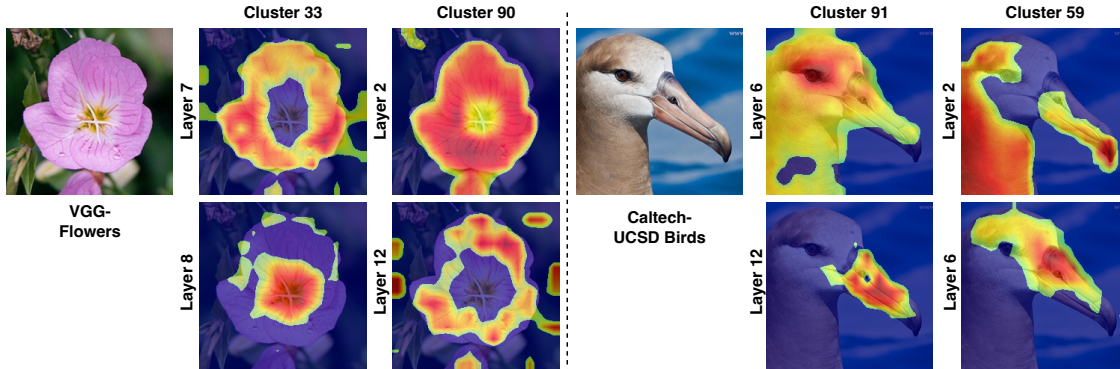
Chinmay Savadikar¹Xi Song²Tianfu Wu¹¹Department of ECE, North Carolina State University, ²An Independent Researcher<https://savadikarc.github.io/gift>

Figure 1. *Flowers, Birds and here are our GIFTs.* Our proposed GIFT is a deep parameter-residual learning method using a generator network for parameter-efficient fine-tuning. In training, given pretrained weights of a layer $\omega \in \mathbb{R}^{d_{out} \times d_{in}}$ in the pretrained backbone, the fine-tuned weights by our GIFT is $\omega^+ = \omega + \text{GIFT}(\omega)$ with learned clustering $\mathcal{C}_{d_{out}, M}$ for the parameters ω , where M is a predefined small number (e.g., 96). In testing, $\mathcal{C}_{d_{out}, M}$ plays the role of a semantic segmentation head classifier. For a testing data x (e.g., a flower image in the VGG Flowers dataset, or a bird in the Caltech-UCSD birds dataset), its output at the given layer is $f(x; \omega^+) \in \mathbb{R}^{h \times w \times d_{out}}$ whose “ M -cluster segmentation results” are simply $f(x; \omega^+) \cdot \mathcal{C}_{d_{out}, M} \in \mathbb{R}^{h \times w \times M}$. Semantically meaningful segmentation maps are observed to emerge (more in Fig. 4 and the Appendix) with object-part like hierarchical relationships between different layers of a same cluster, e.g., cluster 33 in the second column and cluster 91 in the last second column. The effects of $\mathcal{C}_{d_{out}, M}$ are contributed by the top-down attention steering from the gradient back-propagation in training, although it is learned in the parameter space and never directly interacts with the data activation in the forward computation (see Fig. 3). See text for details.

Abstract

We present GIFT (Generative Interpretable Fine-tuning Transformers) for fine-tuning pretrained (often large) Transformer models at downstream tasks in a parameter-efficient way with built-in interpretability. Our GIFT is a deep parameter-residual learning method, which addresses two problems in fine-tuning a pretrained Transformer model: Where to apply the parameter-efficient fine-tuning (PEFT) to be extremely lightweight yet sufficiently expressive, and How to learn the PEFT to better exploit the knowledge of the pretrained model in a direct way? For the former, we select the final projection (linear) layer in the multi-head self-attention of a Transformer model, and verify its effectiveness. For the latter, in contrast to the prior art that directly introduce new model parameters (often in low-rank approximation form) to be learned in fine-tuning with downstream data, we propose a method for learning to generate the fine-tuning parameters. Our GIFT is a hyper-

Transformer which take as input the pretrained parameters of the projection layer to generate its fine-tuning parameters using a proposed Parameter-to-Cluster Attention (PaCa). The PaCa results in a simple clustering-based forward explainer that plays the role of semantic segmentation in testing. In experiments, our proposed GIFT is tested on the VTAB benchmark and the fine-grained visual classification (FGVC) benchmark. It obtains significantly better performance than the prior art. Our code is available at <https://github.com/savadikarc/gift>.

1. Introduction

Fine-tuning pretrained deep neural networks (DNNs) as feature backbones for downstream tasks, often known as transfer learning, has been an important and challenging research topic in the computer vision and deep learning literature ever since the recent resurgence of DNNs pioneered by the AlexNet [25] trained on the ImageNet-1k dataset [41] in

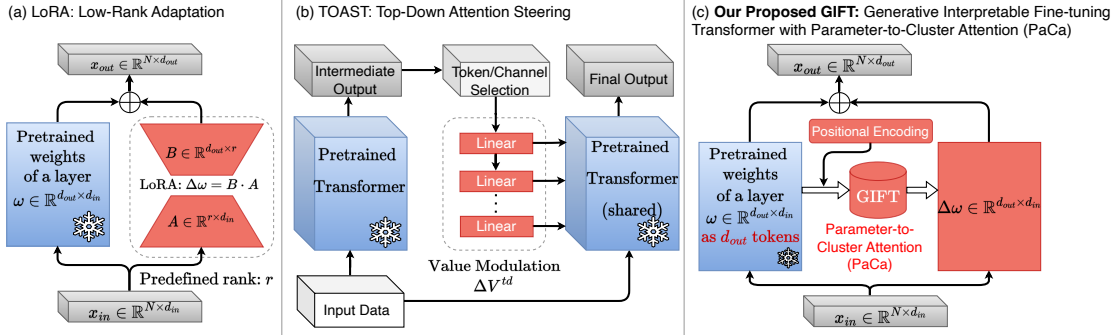


Figure 2. Illustration of our proposed GIFT in comparison with LoRA [19] and TOAST [44]. Both LoRA and our GIFT work at the layer level in the sense that they can be placed to update any selected layers, while TOAST is holistic by learning the value modulation based on the output of the entire frozen backbone. LoRA and our GIFT are more efficient in inference than TOAST since the parameter updates can be merged into the backbone after training. Compared with LoRA, our GIFT is conceptually different. LoRA learns the low-rank parameters A and B by directly treating them as model parameters to optimize (and might entail searching the rank r), while our GIFT takes the parameters of the pretrained backbone as input and outputs the full parameter matrix without resorting to the search of the low rank. To address the quadratic complexity of vanilla Transformers and for efficiency, inspired by the recently proposed Patch-to-Cluster Attention (PaCa) in the PaCa-ViTs [11], we develop a Parameter-to-Cluster Attention (also termed as PaCa). The GIFT is shared by different layers of the pretrained backbone in training.

2012. The goal of fine-tuning DNNs is to transfer knowledge from the pretrained domain/task to facilitate better performance on downstream tasks which otherwise may suffer from not being able to train those DNNs from scratch well due to various considerations such as insufficient amount of data. Fine-tuning DNNs has become a golden standard in practice and shown tremendous and remarkable progress.

To achieve better transferrability, fine-tuning DNNs is not always straightforward by simply updating parameters of a pretrained DNN via gradient back-propagation using a downstream task data (i.e., full fine-tuning). There are subtle details that matter in terms of balancing the exploitation of the pretrained model and the exploration of the new task data [26]: which parts of a pretrained DNN should be fine-tuned, and how should they be trained? These details become explicitly important in continual (or lifelong) learning where addressing catastrophic forgetting is one of the key factors at streaming tasks [34, 45]. More recently, larger and larger feature backbones, so-called large foundation models [3], have become ubiquitous, while hindering the possibility of training them from scratch, and of fine-tuning them as their entirety for researchers and practitioners who do not have access to high-demanding computing resources. In the meanwhile, it may not be even necessary to fine-tune the pretrained model as its entirety due to the aforementioned exploitation-exploration trade-off. To address this issue, parameter-efficient fine-tuning (PEFT) becomes necessary and remains an active research topic.

In this paper, we focus on PEFT of pretrained Transformer models [46], for which the low-rank adaptation (LoRA) [19] is the state-of-the-art method with many follow-up works. Another more recent work is the top-down attention steering (TOAST) method [44]. As illus-

trated in Fig. 2, LoRA learns new model parameters in the low-rank form in fine-tuning and is applicable to different types of DNNs. TOAST learns data-specific value modulation to be added to the value projection in the multi-head self-attention, and thus is mainly specific to the Transformer model. We are motivated by LoRA, but take a conceptually different perspective to PEFT. The low-rank parameters (e.g., A and B) in LoRA are introduced directly as new model parameters in fine-tuning, which do not have direct “information exchange” with the pretrained weights and entails searching the rank r in the adaptation for better performance. We ask the question: **Can we directly learn the fine-tuning parameters from the pretrained weights?** It makes intuitive sense since the pretrained weights “summarize/compress” the data in the pretraining at its corresponding level (e.g., lower layers of a pretrained vision backbone may reflect low-level vision features/patterns). In the literature, methods similar in spirit have been proposed as the so-called hyper-network learning approach [12] which utilize one network to predict the parameters for another network or some of its modules.

In this paper, we present Generative Interpretable Fine-tuning Transformer (GIFT), as illustrated in Fig. 2 (c), to facilitate direct “information exchange” between pretrained weights and fine-tuning ones. At a high-level, our GIFT is a hyper-Transformer to transform a pretrained backbone Transformer better on downstream tasks by directly exploiting the pretrained weights. With GIFT, we have another problem to address: Where to apply GIFT to be sufficiently efficient yet highly expressive? For example, LoRA is often applied to the Query, Key and Value projection layers in Transformers [46]. TOAST specifically modulates the Value activation [44] (see Fig. 2 (b)). Motivated by a recent

work on resilient lifelong learning, which learns to grow artificial hippocampi (ArtiHippo) at the final projection (linear) layers of multi-head self-attention (MHSA) modules in Vision Transformers (ViTs) [42], we follow their observation and apply our GIFT to the final project layer. We verify its effectiveness in experiments.

Our GIFT possesses several advantages: We can build many small GIFTs on top of a shared pretrained model for different downstream tasks, and thus reducing the storage requirement and task-switching overhead. During training, we only need to train the lightweight GIFT, which is very efficient and applicable with consumer GPUs. After training, the learned fine-tuning parameters can be absorbed into the frozen pretrained parameters, and thus with no inference latency introduced. Last, but not least, the parameter-to-cluster attention (PaCa) in our proposed GIFT facilitates interpretable models after fine-tuning as a by-product, which realizes the top-down attention steering [44] in a more effective way and potentially relates to the hierarchical predictive coding principle [21, 23] observed in neuroscience.

2. Related Work and Our Contributions

Hypernetworks. Ha *et al.* [12] introduced Hypernetworks, i.e., neural networks that generate the parameters for other neural networks, in language modelling tasks by generating the weights of an LSTM [15]. Hypernetworks have previously been applied for few-shot classification [56, 57], transfer learning [39] and continual learning [48, 51].

Similar to our proposed approach, [39] learns to adapt a global feature extractor through an adaptation network. However, they use a separate global feature extractor to extract features from images. In a few shot continual learning setup, [47] uses a hyper-Transformer to generate the parameters for a separate Convolutional Neural Network (ConvNet), which use as inputs both a support set of images of the current task and the ConvNet parameters generated for the previous tasks. Although similar to our approach, the hyper-Transformer in [47] still takes the raw data as the input together with the previous parameters. Our proposed GIFT exclusively operates in the parameter space and uses the pretrained parameters of the backbone to adapt the backbone itself for a downstream task. HyperFormer++ [32], which uses a Multi-Layer Perceptron (MLP) to generate the parameters from layer embedding and a latent vector for Adapters [18] introduced across layers of a pretrained model in a multitask setting, comes closest to our approach. Unlike [32], we directly use the weights of the frozen pretrained model itself, thus eliminating the need for layer embeddings. Our GIFT also facilitates capturing the relationship between, and accordingly clustering together, the feature dimensions of the pretrained model across layers, which leads to better interpretability by forming semantic segmentation-like maps as by-products for testing images.

Parameter Efficient Fine-tuning (PEFT). The goal of PEFT methods is to reduce the computational resources (memory footprint, wall time, etc.) required for fine-tuning large models such as Transformers [46] and Vision Transformers (ViTs) [9]. PEFT methods can be divided into two main categories: i) prompt-based methods that keep the backbone model frozen while learning “prompts” that are appended to the data tokens, and ii) fine-tuning methods that introduce new parameters into the frozen backbone either as new injected layers or as parameter-residuals to the selected layers. Prompt-based methods either append prompts to the input tokens [20, 27], or the intermediate layers [28, 30, 54]. Early work on PEFT used sequential/parallel learnable adapters added after the Multi-Head Self Attention and/or FFN blocks [2, 5, 18, 31, 36, 37, 40]. LoRA [19] and its variants [8, 22, 29, 53] use a low-rank factorization of the weight matrices in the linear layers and add the newly learned weights to the frozen weights of the backbone, removing the added inference cost in adapter based methods. Low rank factorization has also been applied for multi-modal models [50]. A combination of all these PEFT methods has also been proposed [4, 13, 33, 55]. Our work draws inspiration from the parameter-residual fine-tuning methods such as LoRA, but leverages hypernetworks to be more generic.

Our Contributions. This paper makes three main contributions in the field of PEFT, especially for pretrained Transformer backbones:

- It presents GIFT (Generative Interpretable Fine-Tuning Transformer), a deep parameter-residual learning method that utilizes a hyper-Transformer purely in the parameter space with an efficient parameter-to-cluster attention (PaCa) of linear complexity.
- The proposed GIFT facilitates learning parameter clusters in the parameter space via PaCa, which are interpretable when projected onto the feature space, and can play the role of semantic segmentation in the sense that different clusters can focus on different parts of the image, even though the images are never passed through GIFT.
- The proposed GIFT achieves better performance than the prior art of PEFT on two benchmarks (VTAB and fine-grained classification). As the pretrained model gets stronger, the performance of our GIFT increases proportionally, unlike the prior art, which is a desirable property for PEFT with large foundation models.

3. Approach

In this section, we first overview the problem formulation of PEFT, and then present details of our proposed GIFT.

3.1. Problem Formulation of PEFT

Denote by Ω the set of parameters of a pretrained backbone model such as the ViT-B [9] pretrained on the ImageNet-

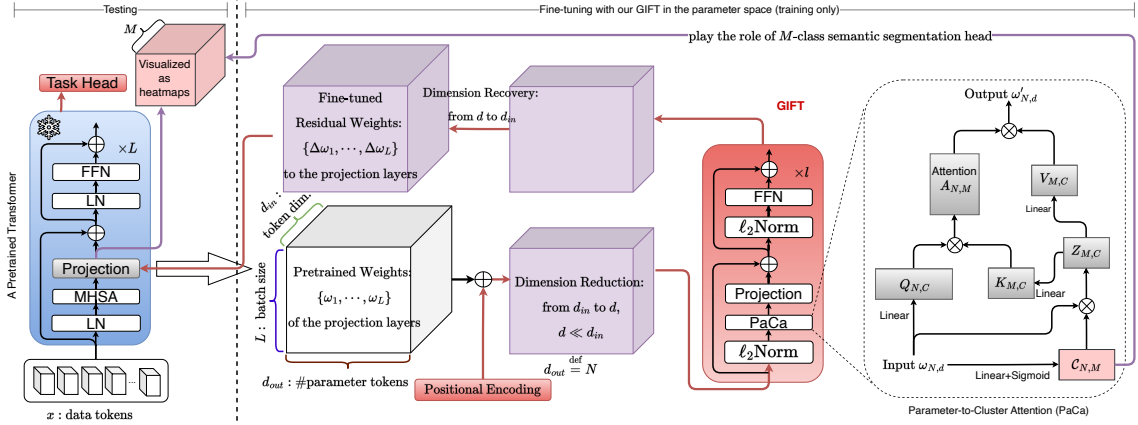


Figure 3. Detailed workflow of our proposed l -layer GIFT for fine-tuning a pretrained and frozen L -layer Transformer backbone on a downstream task. For simplicity we assume the pretrained Transformer is isotropic and thus $d_{out} = d_{in}$ where the subscripts are used to indicate the order. The task head is trained from scratch for the downstream task. See text for details.

21k [41], which will be frozen throughout fine-tuning. Without loss of generality, denote by $\omega \subset \Omega$ the pretrained weights of a certain (primitive) layer in the backbone, $f(\cdot; \omega)$, such as a linear layer or a convolution layer depending on the type of the backbone. Consider a linear layer (ω, b) , we have $\omega \in \mathbb{R}^{d_{out} \times d_{in}}$, where d_{out} and d_{in} are the output and input dimension respectively, and $b \in \mathbb{R}^{d_{out}}$ the bias term. Given an input $x_{in} \in \mathbb{R}^{d_{in}}$, We compute the output by,

$$x_{out} = f(x_{in}; \omega, b) = \omega \cdot x_{in} + b, \quad (1)$$

where $x_{out} \in \mathbb{R}^{d_{out}}$.

For a downstream task, the goal of fine-tuning is to learn the updated parameters ω^+ using the task data (for simplicity we leave the bias b unchanged). In PEFT such as the LoRA method [19] (see Fig. 2 (a)), one popular formulation is to adopt the additive form of updating parameters,

$$\omega^+ = \omega + \Delta\omega, \quad (2)$$

where $\Delta\omega$ is often assumed to be a product of two low-rank parameter matrices $A \in \mathbb{R}^{r \times d_{in}}$ and $B \in \mathbb{R}^{d_{out} \times r}$,

$$\Delta\omega = B \cdot A, \quad (3)$$

where r represents the predefined rank (e.g., $r = 4$). Both A and B are treated as model parameters to be learned via optimizing the objective function defined on the downstream task data (e.g., the cross-entropy loss for classification problems). The total number of learnable parameters in $\Delta\omega$ is much smaller than that of the frozen pretrained weights ω since both d_{in} and d_{out} are often much larger than the predefined low rank r .

To be really efficient in practice, we also need to specify where to apply PEFT in a given pretrained model, which itself is often treated as hyper-parameter tuning with the goal to select a subset of layers to balance the trade-off between efficiency and expressivity (i.e., performance on the downstream task). The same is for the rank r .

3.2. Our Proposed GIFT

Our GIFT generalizes the parameterization scheme in Eqn. 3 by learning a parameter generator network,

$$\Delta\omega = g(\omega; \theta), \quad (4)$$

where θ is the set of parameters of the generator network to be trained using a downstream task data.

With this generative formulation, we do not need to assume the low-rank form as in Eqn. 3 (which is a specific case of Eqn. 4). Thanks to the expressive power of generator networks, we could learn better adaptation, as we shall see the comparisons in experiments. And, the parameter-residual $\Delta\omega$ is directly driven by the pretrained weights ω .

The input space to the generator network $g(\cdot; \theta)$ is the pretrained weights of a given backbone which is frozen throughout fine-tuning. We do not have “good” inductive bases to exploit in parameterizing $g(\cdot; \theta)$ itself. So, we leverage the expressive modeling power of Transformers [46], resulting in the proposed GIFT.

Consider the input $\omega \in \mathbb{R}^{d_{out} \times d_{in}}$, we treat it as d_{out} tokens each of which is d_{in} -dim vector. For fine-tuning multiple layers of a pretrained backbone (e.g., L layers), the set of their parameters, $\{\omega_l\}_{l=1}^L$, will be treated as the batch of input data to $g(\cdot; \theta)$. Our GIFT consists of four components (Fig. 3):

- *The Positional Encoding Layer:* Due to the permutation invariance nature of Transformers, we introduce a learnable positional encoding vector, $\theta_0 \in \mathbb{R}^{d_{out} \times d_{in}}$ as typically done in training Transformers,

$$\omega^{(1)} = \omega + \theta_0. \quad (5)$$

- *The Dimension Reduction Layer:* Considering that DNNs are often overparameterized and for the sake of efficiency and lightness, we reduce the input dimension d_{in} of each token to some predefined d -dimension (e.g., $d = 48$) via a linear projection layer,

$$\omega^{(2)} = \text{Linear}(\omega^{(1)}; \theta_1), \quad (6)$$

- *The Transformer Blocks*: There are a number of blocks in our GIFT (e.g., 4) with all the parameters collected in θ_{attn} . It adopts the conventional meta-architecture consisting of token mixing via a multi-head self attention (MHSA) module and channel mixing via a feed-forward network (FFN), both using residual connections,

$$\omega^{(3)} = \omega^{(2)} + \text{MHSA}(\text{Norm}(\omega^{(2)})), \quad (7)$$

$$\omega^{(4)} = \omega^{(3)} + \text{FFN}(\text{Norm}(\omega^{(3)})), \quad (8)$$

where $\text{Norm}(\cdot)$ is the ℓ_2 normalization, different from the LayerNorm [1] typically used in Transformers since the inputs are parameters rather than raw data. The $\text{FFN}(\cdot)$ is the multi-layer perceptron (MLP) with the GELU non-linearity function [14]. The $\text{MHSA}(\cdot)$ is our proposed parameter-to-cluster attention (PaCa) module (Sec. 3.4) to address the quadratic complexity of vanilla Transformers, adapted from the recently proposed patch-to-cluster attention method [11]. We elaborate on the PaCa module in the next subsection.

- *The Dimension Recovery Layer*: To compensate the dimension reduction before the Transformer blocks, we recover the required dimension d_{in} using another linear projection layer. Without the confusion of notations in the context, we still use $\omega^{(4)}$ to denote the output from the final Transformer block. We have the fine-tuning parameters generated,

$$\Delta w = \text{Linear}(\omega^{(4)}; \theta_{\Delta}). \quad (9)$$

In our GIFT, we have trainable parameters, $\theta = (\theta_0, \theta_1, \theta_{attn}, \theta_{\Delta})$, which will be learned using the downstream task data using a standard loss function (e.g., cross-entropy in the case of classification).

3.3. The GIFT for Pretrained Transformers

So far, we describe our GIFT by considering one given (linear) layer for the clarity of presentation. Although it is generically applicable to many different pretrained backbone models, we focus on applying our GIFT to pretrained Transformers due to their increasingly dominance in computer vision and machine learning. One remaining question is where to apply GIFT to be extremely efficient yet sufficiently expressive in fine-tuning the pretrained Transformer backbone for downstream tasks.

To that end, we follow the observation in the ArtiHippo method [42], which identifies the final projection (linear) layer of MHSA to be a sweet spot in transfer learning and lifelong learning (see Fig. 3). We verify its effectiveness in our GIFT experiments for both our GIFT and the LoRA method. So, for L -layer pretrained Transformer backbone (such as the 12-layer ViT-B [9]), we will have L linear layers in total to be fine-tuned using our GIFT.

3.4. PaCa: the Parameter-to-Cluster Attention

The vanilla MHSA module is of quadratic complexity and the number of tokens, d_{out} , in our GIFT is often large, especially for pretrained large models. To deliver the advantages of PEFT, we propose the parameter-to-cluster attention, inspired by the recently proposed patch-to-cluster attention (PaCa) [11]. We use the same shorthand name, PaCa.

The vanilla single-head self-attention for an input sequence of N C -dimensional tokens, $x_{N,C}$ is defined by,

$$z_{N,C} = \text{Softmax}\left(\frac{Q_{N,C} \cdot K_{N,C}^{\top}}{\sqrt{C}}\right) \cdot V_{N,C}, \quad (10)$$

where $Q_{N,C}$, $K_{N,C}$ and $V_{N,C}$ are the Query, Key and Value computed from the input x (often by linear projection layers). The quadratic complexity, $\mathcal{O}(N^2)$, comes from the nominator inside the Softmax. MHSA can be straightforwardly defined on top of Eqn. 10. To address the quadratic complexity while retaining the length of output sequence, one solution is to reduce the length of the Key and the Value to some predefined small number, M (e.g., $M = 96$). We can rewrite Eqn. 10 by,

$$z_{N,C} = \text{Softmax}\left(\frac{Q_{N,C} \cdot K_{M,C}^{\top}}{\sqrt{C}}\right) \cdot V_{M,C}. \quad (11)$$

To that end, a learnable clustering module is presented in [11]. It first computes the cluster assignment for each token by,

$$\mathcal{C}_{N,M} = \text{Softmax}(h(x_{N,C})), \quad (12)$$

where $h(\cdot)$ can be simply a linear projection layer, and the Softmax is applied across the tokens. Then, M clusters are formed by,

$$y_{M,C} = \text{Norm}(\mathcal{C}_{N,M}^{\top} \cdot x_{N,C}), \quad (13)$$

from which the Key, $K_{M,C}$ and the Value, $V_{M,C}$ are computed. Eqn. 13 represents how much each token contributes to a cluster. Hence, each cluster can be thought of as a weighted mixture of tokens.

In our GIFT, we observe that the Softmax in the cluster assignment (Eqn. 12) is not a proper nonlinearity function to use. The objective of applying Softmax in Eqn. 12 in the original PaCa method [11] is to compress the entire input feature map into some potentially meaningful foreground clusters that are important for the task at hand (e.g., image classification). During our development, using Softmax in our GIFT will enforce it to learn almost uniform cluster assignment, i.e., $\mathcal{C}_{n,m} \approx \frac{1}{N}, \forall n, m$. Instead, we utilize the Sigmoid function and we change Eqn. 12 to,

$$\mathcal{C}_{N,M} = \frac{1}{N} \cdot \text{Sigmoid}(h(x_{N,C})), \quad (14)$$

where $\frac{1}{N}$ can be interpreted as the prior, and $\text{Sigmoid}(h(x_{N,C}))$ as the likelihood in assigning clusters to each of $N = d_{out}$ tokens.

Eqn. 14 makes more sense for our GIFT due to the nature of the tokens (i.e., pretrained weights). In the parameter space, especially for the projection layers in MHSA we se-

lect to fine-tune (whose goal is to fuse the information from the split multi-head self-attention), the parameter tokens do not have the foreground/background separation which we typically observe in the data token space for classification tasks. Softmax normalization may overly penalize some tokens by inducing too aggressive competition among the tokens, which may hinder the effectiveness of parameter-residual learning. Our observation of Softmax leading to almost uniform cluster assignment verifies this: if an improper “credit assignment” function is used, to ensure the fine-tuning performance on a downstream task, our GIFT has no choice and must find means of trivializing the “credit assignment” function. A similar argument has been made in the context of attention across the channels of the FFN [59]. Eqn. 14 results in the effects we observed in Fig. 1.

3.5. The Interpretability of GIFT

$\mathcal{C}_{N,M}$ or more precisely $\mathcal{C}_{d_{out},M}$ in Eqn. 14 plays a central role in our GIFT. To understand what information it has “captured” during training GIFT, we utilize $\mathcal{C}_{d_{out},M}$ to map back to the data/activation space to see if some meaningful data/feature clusters can emerge. **We observe surprisingly that $\mathcal{C}_{d_{out},M}$ plays the role of a semantic segmentation head classifier.**

Consider image classification tasks, after training, $\mathcal{C}_{d_{out},M}$ is frozen, and for a testing image of I patch-based tokens, its activation map at a certain layer is defined following Eqn. 1 by,

$$x_{out}^+ = f(x_{in}^+; \omega^+, b), \quad x_{out}^+ \in \mathbb{R}^{I \times d_{out}}. \quad (15)$$

Similar to Eqn. 13, we can compute M cluster assignment maps for the activation,

$$m_{out} = x_{out}^+ \cdot \mathcal{C}_{d_{out},M}, \quad (16)$$

each of the M cluster assignment maps can be visualized as a heatmap to visually check its meaningfulness. Note that the relative values of the clusters $\mathcal{C}_{d_{out},M}$ are more important than the absolute values in Eqn. 13, which represents how much each output dimension contributes to a cluster. Hence, for visualizing the clusters using Eqn. 16, we normalize $\mathcal{C}_{d_{out},M}$ along d_{out} using the mean and standard deviation of a cluster.

As shown in Fig. 1, we can see the cluster assignment maps are sensible across different examples. We note that $\mathcal{C}_{d_{out},M}$ represents how and what our GIFT “sees” an image in the model parameter space during fine-tuning. Its meaningfulness on testing data justifies the interpretability of our proposed GIFT. It can be seen that different clusters attend to different parts in the image (beak/head/body of a bird). Note that this behavior emerges in the parameter clusters even though data activation in the backbone is never directly passed through GIFT in training, and the clustering module only receives the information about data activation through the gradients calculated during backpropagation in training.

3.6. The Interpretability Emerged in our GIFT

To understand how the clustering behavior can occur, consider the gradients of the parameter-residual $\Delta\omega$ with respect to the loss function ℓ (e.g., cross-entropy between the network prediction and the ground-truth) at a certain projection layer $x_{out} = f(x_{in}; \omega^+, b) = (\omega + \Delta\omega) \cdot x_{in} + b$, we have,

$$\nabla_{\Delta\omega} \ell = (\nabla_{x_{out}} \ell) \cdot x_{in}^\top$$

i.e., the gradients received by the parameter-residual $\Delta\omega$ are the matrix product of the top-down information (carried by $\nabla_{x_{out}} \ell$, i.e., the class-activation map [58] at the project layer) and the bottom-up feature information (x_{in}), and thus provide means of measuring the coherence/consistency between the bottom-up and top-down information. Hence, the top-down feedback modulated bottom-up features pass through the GIFT during the backward pass to drive the learning of the clustering module $\mathcal{C}_{d_{out},M}$. With the hyper-Transformer architecture of our GIFT, the clustering module is sufficiently expressive and induced to learn meaningful “segmentation” either to enhance the top-down/bottom-up coherence or to remedy the disagreement between the top-down and the bottom-up.

This mimics the behavior of top-down attention steering [43, 44]. With this intuitive explanation, it is not surprising that the our GIFT can learn attention-like clusters, but without the added cost of an additional forward pass, and without resorting to the token/channel selection in the TOAST [44]. At a high-level, the learning behavior of the clustering module in our GIFT might be related to the hierarchical predictive coding principle in neuroscience [6, 17, 21, 23, 38], which postulates that the higher cortical areas provide top-down feedback in a cooperative, competitive and entangled computation to a feedforward sensory bottom-up process to enable a robust joint inference. Note that parameter-residual methods like LoRA [19] also follow the similar gradients, but their underlying low-rank approximation based representation for w^+ might not be expressive enough to capture the rich semantic information in the top-down signal.

4. Experiments

In this section, our GIFT is tested on two classification benchmarks and outperforms the prior art.

Data and Metric. Two benchmarks are tested. The first is the Visual Task Adaptation Benchmark (VTAB-1k) benchmark [52], which consists of 19 tasks in three super-categories (natural, specialized and structured), drawn from a variety of domains, and with various semantics. The second is the widely used fine-grained visual classification (FGVC) benchmark in transfer learning, containing 5 datasets, consisting of Caltech-UCSD Birds [49], NABirds [16], Oxford Flowers [35], Stanford Cars [10], and Stanford

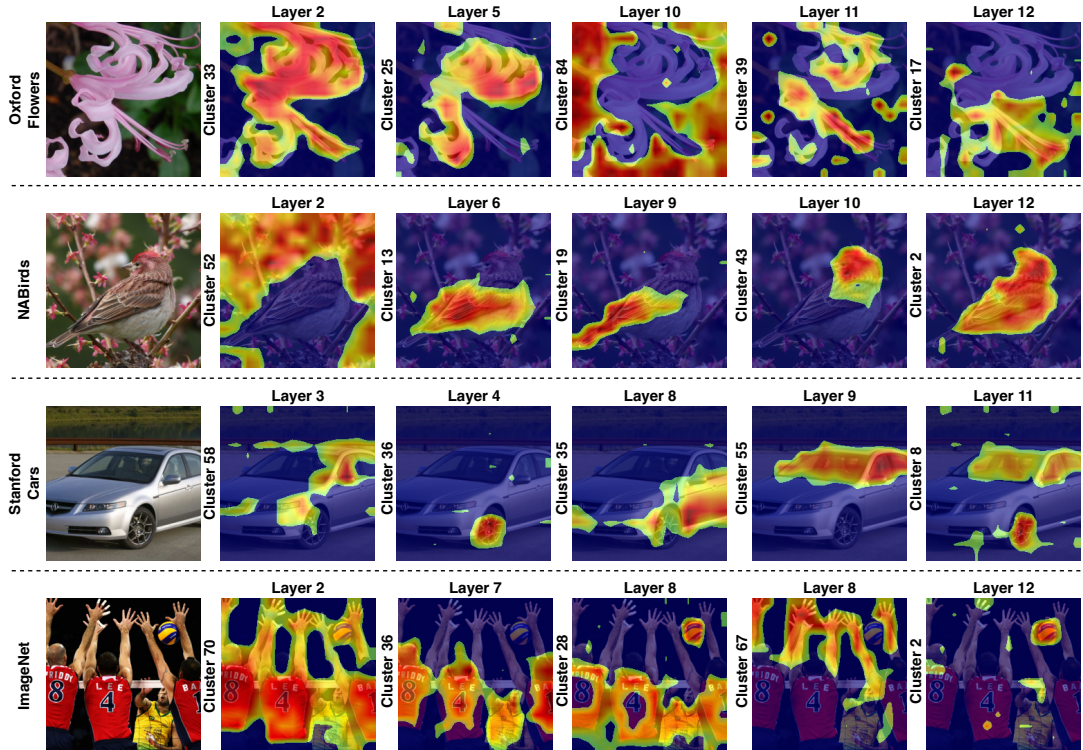


Figure 4. Meaningful clusters consistently emerge after GIFT training on various datasets. From top to bottom, *on Flowers*, GIFT learns to form clusters on the full flower (Layer 2), petals (Layer 5), stamen (Layers 11 and 12). *On NABirds*, clusters are formed on various parts on the bird, such as the full body (Layer 12), head (Layers 10), wing+tail (Layer 9), torso (Layer 6), and even the background (Layer 2). *For Cars*, GIFT learns to form clusters on the door (Layer 8), wheel (Layer 4), windshield (Layer 9), and even a composition of both (Layer 11). *For ImageNet*, clusters on the foreground (Layer 2), players (Layer 7), arms+hands (Layer 8, Cluster 67), ball (Layer 12), and players+ball (Layer 8, Cluster 28) can be seen. Please check more examples in the Appendix.

Method	Comments	Natural							Specialized				Structured							Average	
		C100	C101	DTD	Flwr	Pets	SVHN	Sun397	PCam	ESAT	Res45	D-Reti	Civr-Cnt	Civr-Dst	DMLab	KITTI	dSr-Loc	dSr-Ori	sN-Azim		sN-Ele
ViT-B/16, ImageNet1k																					
Fine-tune*	-	44.7	77.3	55.5	74.5	86	85.1	17.4	84.9	95	82.8	74.2	60.2	53.1	33.5	77.6	61.9	39	15	36.6	60.8
VPT*	-	65.3	90.5	67.7	88.3	88.6	82.2	40.6	82.3	94.5	83.1	74	51.5	51.1	44.1	69.3	63.8	49.5	25.3	28.6	65.3
LoRA (QKV)*	Rank=4	69.3	88.8	66.6	90.3	90.3	81.9	41.5	83.4	94.8	83.5	75	66.8	56.9	48.9	77.6	76.2	53.5	26.6	37.1	68.9
TOAST (V)*	-	73.8	92.1	68.7	93.0	89.0	76.3	41.9	82.8	95.3	85.7	74.6	61.2	58.7	43.5	78.8	86.1	51.2	27.0	43.4	69.6
LoRA (Proj)	Rank=4	68.8	88.2	66.0	89.9	89.8	87.0	41.5	83.3	95.7	78.9	72.1	63.1	52.6	43.1	71.2	67.0	52.2	30.4	32.5	67.0
LoRA (Proj)	Rank=48	62.0	87.7	66.0	85.7	89.9	71.0	41.7	79.7	94.1	77.8	73.3	38.0	48.7	39.3	69.8	58.4	50.3	23.6	27.7	62.3
Our GIFT	Dim=48	74.5	92.0	65.4	92.4	91.4	91.2	43.4	83.3	96.4	84.8	73.6	66.0	54.0	48.9	80.5	70.3	51.6	32.9	31.6	69.7
ViT-B/16, ImageNet21k																					
Fine-tune*	-	70.2	85.8	64.3	97.5	85.8	85.9	40.0	78.2	95.7	83.8	73.9	53.1	57.3	37.5	68.2	60.5	35.2	18.8	28.0	64.2
VPT*	-	75.4	88.7	66.3	98.1	87.3	73.7	52.3	80.3	93.5	83.4	74.1	49.6	58.1	41.9	62.7	65.1	42.9	24.0	24.2	65.4
LoRA (QKV)*	Rank=4	83.6	89.4	66.2	98.6	89.4	83.8	52.6	81.1	95.8	84.6	74.7	77.6	59.5	46.8	74.1	73.0	48.6	25.6	32.2	70.4
TOAST (V)*	-	82.1	90.5	70.5	98.7	89.7	71.9	53.3	84.3	95.5	85.5	74.2	75.4	60.8	44.7	77.5	73.9	47.5	24.5	33.7	70.2
LoRA (Proj)	Rank=4	83.7	91.5	71.2	98.2	90.7	86.1	54.1	83.8	95.7	84.0	73.9	77.5	58.5	49.6	74.1	62.5	48.7	27.5	34.8	70.8
LoRA (Proj)	Rank=48	74.3	87.9	65.9	98.0	87.1	53.2	51.3	80.8	92.4	76.6	74.4	54.0	32.6	35.0	64.7	53.2	39.7	15.2	24.7	61.1
Our GIFT	Dim=48	82.0	91.5	70.0	98.9	90.9	90.3	52.4	84.5	96.2	83.6	71.7	76.7	60.8	48.8	77.9	76.2	49.5	33.1	35.0	72.1

Table I. Results on the VTAB-1k benchmark [52]. The “Dim” for GIFT refers to the dimension of the features in the hyper-Transformer. * indicates that results are obtained from [44].

Dogs [24]. Top-1 accuracy is used in evaluation.

Pretrained Models and Baseline Methods. We compare our GIFT with Visual Prompt Tuning (VPT) [20], LoRA [19], and Top-Down Attention Steering (TOAST) [44] using ViT-B/16 as the backbone model. On the

VTAB-1k benchmark, we use the backbone pretrained on ImageNet-21k [7] (using supervised training) and ImageNet1k [41]. On the fine-grained classification benchmark, we use the ViT-B/16 backbone pretrained on ImageNet-1k [41]. **Due to space limit, we provide the im-**

Method	Comments	CUB	NABirds	Oxford Flower	Stanford Dogs	Stanford Cars	Average
Linear*	-	76.8	47.3	81.7	97.7	60.3	72.8
Fine-tune*	-	80.5	60.2	86.9	94.7	83.2	81.1
VPT*	-	76.9	72.2	80.6	97.3	62.8	78.0
LoRA (QKV)*	Rank=4	82.5	71.2	81.2	97.5	76.6	79.8
TOAST (V)*	-	85.0	75.2	88.7	97.4	84.9	86.2
LoRA (Proj)	Rank=4	81.8	76.3	92.5	97.8	81.4	86.0
LoRA (Proj)	Rank=48	77.8	73.1	88.1	97.6	74.4	82.2
Our GIFT	Dim=192	85.3	82.0	94.0	97.5	87.7	89.3

Table 2. Results on finegrained classification tasks using ViT-B/16 backbone pretrained on ImageNet1k. The ‘‘Dim’’ for GIFT refers to the dimension of the features in the hyper-Transformer. * indicates that results are obtained from [44].

plementation details in the Appendix.

4.1. Results

VTAB-1k: As shown in Table 1, our GIFT performs better than all the other methods. Notably, the performance of our GIFT improves substantially with a stronger pretrained backbone (ViT-B/16 pretrained on ImageNet21k) while other methods show marginal gains. This shows that our method can better leverage stronger backbones, since our method learns to fine-tune directly in the parameter space of pretrained backbones. A stronger parameter space will naturally lead to better performance.

FGVC: As shown in Table 2, our GIFT outperforms the baselines by a large margin, which shows the quantitative effectiveness of our method. The gain is particularly high for the NABirds dataset, which contains 555 classes, suggesting that our method scales better with the data complexity and size than other compared methods. Furthermore, as shown in Figure 4, our method can form meaningful and diverse clusters when projected from parameter space onto the feature space. Compared with the runner-up method, TOAST (V), our GIFT is twice as efficient in inference while being significantly better (3.1% improvement)

Observations on LoRA: On both the benchmarks, LoRA is sensitive to the rank r , and increasing the rank degrades the performance. Our GIFT is observed to be robust.

The Effectiveness of the Projection Layer in MHSA for PEFT. On the VTAB-1K benchmark, with the stronger ImageNet-21k trained backbone, LoRA (Proj) works slightly better than LoRA (QKV), 70.8 vs 70.4, as well as TOAST (V). On the FGVC benchmark, LoRA (proj) works significantly better than LoRA (QKV), 86.0 vs 79.8. In both cases, LoRA (proj) uses less fine-tuned parameters. These verify the effectiveness of the selection of the projection layer as the sweet spot in PEFT, adopted from [42].

4.2. Ablation Studies

The FGVC datasets, on which we test the clustering behavior, are specialized datasets of relatively small scale. A natural question to ask is if a similar clustering behavior can occur on a more diverse dataset like the ImageNet1k [41]. To test this, we treat the ImageNet1k as just another ‘‘downstream’’ task and train our GIFT the same way as done for

other datasets in the FGVC benchmark using the frozen ImageNet1k trained backbone. As seen in Figure 4, our GIFT can learn to form clusters even on a large scale dataset, hinting towards the generic nature of our method beyond fine-tuning. Note that this behavior occurs even if we train GIFT for only 2 epochs (1 warmup epoch). This clearly shows the effectiveness of the PaCa module in our GIFT. Please see the Appendix for more visualizations of the learned clusters on the ImageNet1k.

5. Conclusion

We propose Generative Interpretable Fine-Tuning Transformer (GIFT), a deep parameter-residual learning method that directly uses the pretrained weights of a backbone as tokens to learn to generate the finetuning parameter-residuals using a hyper-Transformer. We also present a Parameter-to-Cluster Attention (PaCa) module in our GIFT, which learns to cluster the parameter tokens for efficiency. The learned clusters can be mapped back to the feature (data) space to form diverse and meaningful segmentation-like maps on the data space, showing the built-in interpretability of our GIFT. In experiments, we show that our GIFT can perform efficient finetuning in a low-data regime, as evidenced by our strong performance on the VTAB-1k benchmark, and its performance scales proportionally to the strength of the underlying pretrained model. On the FGVC benchmark, we show that our GIFT can scale better as the data complexity and size increases, as compared to other baselines.

Acknowledgements

This research is partly supported by NSF IIS-1909644, ARO Grant W911NF1810295, ARO Grant W911NF2210010, NSF IIS-1822477, NSF CMMI-2024688, NSF IUSE-2013451 and DHHS-ACL Grant 90IFDV0017-01-00. The views and conclusions contained herein are those of the authors and should not be interpreted as necessarily representing the official policies or endorsements, either expressed or implied, of the NSF, ARO, DHHS or the U.S. Government. The U.S. Government is authorized to reproduce and distribute reprints for Governmental purposes not withstanding any copyright annotation thereon.

References

- [1] Lei Jimmy Ba, Jamie Ryan Kiros, and Geoffrey E. Hinton. Layer normalization. *CoRR*, abs/1607.06450, 2016. [5](#)
- [2] Ankur Bapna and Orhan Firat. Simple, scalable adaptation for neural machine translation. In *Proceedings of the 2019 Conference on Empirical Methods in Natural Language Processing and the 9th International Joint Conference on Natural Language Processing, EMNLP-IJCNLP 2019, Hong Kong, China, November 3-7, 2019*, pages 1538–1548. Association for Computational Linguistics, 2019. [3](#)
- [3] Rishi Bommasani, Drew A Hudson, Ehsan Adeli, Russ Altman, Simran Arora, Sydney von Arx, Michael S Bernstein, Jeannette Bohg, Antoine Bosselut, Emma Brunskill, et al. On the opportunities and risks of foundation models. *arXiv preprint arXiv:2108.07258*, 2021. [2](#)
- [4] Arnav Chavan, Zhuang Liu, Deepak K. Gupta, Eric P. Xing, and Zhiqiang Shen. One-for-all: Generalized lora for parameter-efficient fine-tuning. *CoRR*, abs/2306.07967, 2023. [3](#)
- [5] Shoufa Chen, Chongjian Ge, Zhan Tong, Jiangliu Wang, Yibing Song, Jue Wang, and Ping Luo. Adaptformer: Adapting vision transformers for scalable visual recognition. In *NeurIPS*, 2022. [3](#)
- [6] Andy Clark. Whatever next? predictive brains, situated agents, and the future of cognitive science. *Behavioral and brain sciences*, 36(3):181–204, 2013. [6](#)
- [7] Jia Deng, Wei Dong, Richard Socher, Li-Jia Li, Kai Li, and Li Fei-Fei. Imagenet: A large-scale hierarchical image database. In *2009 IEEE Computer Society Conference on Computer Vision and Pattern Recognition (CVPR 2009), 20-25 June 2009, Miami, Florida, USA*, pages 248–255. IEEE Computer Society, 2009. [7](#), [12](#)
- [8] Tim Dettmers, Artidoro Pagnoni, Ari Holtzman, and Luke Zettlemoyer. Qlora: Efficient finetuning of quantized llms. *CoRR*, abs/2305.14314, 2023. [3](#)
- [9] Alexey Dosovitskiy, Lucas Beyer, Alexander Kolesnikov, Dirk Weissenborn, Xiaohua Zhai, Thomas Unterthiner, Mostafa Dehghani, Matthias Minderer, Georg Heigold, Sylvain Gelly, Jakob Uszkoreit, and Neil Houlsby. An image is worth 16x16 words: Transformers for image recognition at scale. In *9th International Conference on Learning Representations, ICLR 2021, Virtual Event, Austria, May 3-7, 2021*. OpenReview.net, 2021. [3](#), [5](#), [12](#)
- [10] Timnit Gebru, Jonathan Krause, Yilun Wang, Duyun Chen, Jia Deng, and Li Fei-Fei. Fine-grained car detection for visual census estimation. In *Proceedings of the Thirty-First AAAI Conference on Artificial Intelligence, February 4-9, 2017, San Francisco, California, USA*, pages 4502–4508. AAAI Press, 2017. [6](#), [12](#), [13](#)
- [11] Ryan Grainger, Thomas Paniagua, Xi Song, Naresh Cuntoor, Mun Wai Lee, and Tianfu Wu. Paca-vit: Learning patch-to-cluster attention in vision transformers. In *Proceedings of the IEEE/CVF Conference on Computer Vision and Pattern Recognition (CVPR)*, pages 18568–18578, 2023. [2](#), [5](#)
- [12] David Ha, Andrew M. Dai, and Quoc V. Le. HyperNetworks. In *International Conference on Learning Representations*, 2016. [2](#), [3](#)
- [13] Junxian He, Chunting Zhou, Xuezhe Ma, Taylor Berg-Kirkpatrick, and Graham Neubig. Towards a unified view of parameter-efficient transfer learning. In *The Tenth International Conference on Learning Representations, ICLR 2022, Virtual Event, April 25-29, 2022*. OpenReview.net, 2022. [3](#)
- [14] Dan Hendrycks and Kevin Gimpel. Gaussian error linear units (gelus). *arXiv preprint arXiv:1606.08415*, 2016. [5](#)
- [15] Sepp Hochreiter and Jürgen Schmidhuber. Long short-term memory. *Neural Comput.*, 9(8):1735–1780, 1997. [3](#)
- [16] Grant Van Horn, Steve Branson, Ryan Farrell, Scott Haber, Jessie Barry, Panos Ipeirotis, Pietro Perona, and Serge J. Belongie. Building a bird recognition app and large scale dataset with citizen scientists: The fine print in fine-grained dataset collection. In *IEEE Conference on Computer Vision and Pattern Recognition, CVPR 2015, Boston, MA, USA, June 7-12, 2015*, pages 595–604. IEEE Computer Society, 2015. [6](#), [13](#)
- [17] Toshihiko Hosoya, Stephen A Baccus, and Markus Meister. Dynamic predictive coding by the retina. *Nature*, 436(7047): 71–77, 2005. [6](#)
- [18] Neil Houlsby, Andrei Giurgiu, Stanislaw Jastrzebski, Bruna Morrone, Quentin de Laroussilhe, Andrea Gesmundo, Mona Attariyan, and Sylvain Gelly. Parameter-efficient transfer learning for NLP. In *Proceedings of the 36th International Conference on Machine Learning, ICML 2019, 9-15 June 2019, Long Beach, California, USA*, pages 2790–2799. PMLR, 2019. [3](#)
- [19] Edward J Hu, yelong shen, Phillip Wallis, Zeyuan Allen-Zhu, Yuanzhi Li, Shean Wang, Lu Wang, and Weizhu Chen. LoRA: Low-rank adaptation of large language models. In *International Conference on Learning Representations*, 2022. [2](#), [3](#), [4](#), [6](#), [7](#), [12](#)
- [20] Menglin Jia, Luming Tang, Bor-Chun Chen, Claire Cardie, Serge J. Belongie, Bharath Hariharan, and Ser-Nam Lim. Visual prompt tuning. In *Computer Vision - ECCV 2022 - 17th European Conference, Tel Aviv, Israel, October 23-27, 2022, Proceedings, Part XXXIII*, pages 709–727. Springer, 2022. [3](#), [7](#)
- [21] Linxing Preston Jiang and Rajesh PN Rao. Predictive coding theories of cortical function. *arXiv preprint arXiv:2112.10048*, 2021. [3](#), [6](#)
- [22] Shibo Jie and Zhi-Hong Deng. Fact: Factor-tuning for lightweight adaptation on vision transformer. In *Thirty-Seventh AAAI Conference on Artificial Intelligence, AAAI 2023, Thirty-Fifth Conference on Innovative Applications of Artificial Intelligence, IAAI 2023, Thirteenth Symposium on Educational Advances in Artificial Intelligence, EAAI 2023, Washington, DC, USA, February 7-14, 2023*, pages 1060–1068. AAAI Press, 2023. [3](#)
- [23] Georg B Keller and Thomas D Mrsic-Flogel. Predictive processing: a canonical cortical computation. *Neuron*, 100(2): 424–435, 2018. [3](#), [6](#)
- [24] Aditya Khosla, Nityananda Jayadevaprakash, Bangpeng Yao, and Li Fei-Fei. Novel dataset for fine-grained image categorization. In *First Workshop on Fine-Grained Visual Categorization, IEEE Conference on Computer Vision and Pattern Recognition*, Colorado Springs, CO, 2011. [7](#), [13](#)

- [25] Alex Krizhevsky, Ilya Sutskever, and Geoffrey E Hinton. Imagenet classification with deep convolutional neural networks. In *Advances in Neural Information Processing Systems*. Curran Associates, Inc., 2012. 1
- [26] Yoonho Lee, Annie S Chen, Fahim Tajwar, Ananya Kumar, Huaxiu Yao, Percy Liang, and Chelsea Finn. Surgical fine-tuning improves adaptation to distribution shifts. *arXiv preprint arXiv:2210.11466*, 2022. 2
- [27] Brian Lester, Rami Al-Rfou, and Noah Constant. The power of scale for parameter-efficient prompt tuning. In *Proceedings of the 2021 Conference on Empirical Methods in Natural Language Processing, EMNLP 2021, Virtual Event / Punta Cana, Dominican Republic, 7-11 November, 2021*, pages 3045–3059. Association for Computational Linguistics, 2021. 3
- [28] Xiang Lisa Li and Percy Liang. Prefix-tuning: Optimizing continuous prompts for generation. In *Proceedings of the 59th Annual Meeting of the Association for Computational Linguistics and the 11th International Joint Conference on Natural Language Processing, ACL/IJCNLP 2021, (Volume 1: Long Papers), Virtual Event, August 1-6, 2021*, pages 4582–4597. Association for Computational Linguistics, 2021. 3
- [29] Vladislav Lialin, Namrata Shivagunde, Sherin Muckatira, and Anna Rumshisky. Stack more layers differently: High-rank training through low-rank updates. *CoRR*, abs/2307.05695, 2023. 3
- [30] Xiao Liu, Kaixuan Ji, Yicheng Fu, Zhengxiao Du, Zhilin Yang, and Jie Tang. P-tuning v2: Prompt tuning can be comparable to fine-tuning universally across scales and tasks. *CoRR*, abs/2110.07602, 2021. 3
- [31] Rabeeh Karimi Mahabadi, James Henderson, and Sebastian Ruder. Compacter: Efficient low-rank hypercomplex adapter layers. In *Advances in Neural Information Processing Systems 34: Annual Conference on Neural Information Processing Systems 2021, NeurIPS 2021, December 6-14, 2021, virtual*, pages 1022–1035, 2021. 3
- [32] Rabeeh Karimi Mahabadi, Sebastian Ruder, Mostafa Dehghani, and James Henderson. Parameter-efficient multi-task fine-tuning for transformers via shared hypernetworks. In *Proceedings of the 59th Annual Meeting of the Association for Computational Linguistics and the 11th International Joint Conference on Natural Language Processing, ACL/IJCNLP 2021, (Volume 1: Long Papers), Virtual Event, August 1-6, 2021*, pages 565–576. Association for Computational Linguistics, 2021. 3
- [33] Yuning Mao, Lambert Mathias, Rui Hou, Amjad Almahairi, Hao Ma, Jiawei Han, Scott Yih, and Madian Khabsa. Unipelt: A unified framework for parameter-efficient language model tuning. In *Proceedings of the 60th Annual Meeting of the Association for Computational Linguistics (Volume 1: Long Papers), ACL 2022, Dublin, Ireland, May 22-27, 2022*, pages 6253–6264. Association for Computational Linguistics, 2022. 3
- [34] Michael McCloskey and Neal J Cohen. Catastrophic interference in connectionist networks: The sequential learning problem. In *Psychology of learning and motivation*, pages 109–165. Elsevier, 1989. 2
- [35] Maria-Elena Nilsback and Andrew Zisserman. Automated flower classification over a large number of classes. In *Sixth Indian Conference on Computer Vision, Graphics & Image Processing, ICVGIP 2008, Bhubaneswar, India, 16-19 December 2008*, pages 722–729. IEEE Computer Society, 2008. 6, 13
- [36] Jonas Pfeiffer, Ivan Vulic, Iryna Gurevych, and Sebastian Ruder. MAD-X: an adapter-based framework for multi-task cross-lingual transfer. In *Proceedings of the 2020 Conference on Empirical Methods in Natural Language Processing, EMNLP 2020, Online, November 16-20, 2020*, pages 7654–7673. Association for Computational Linguistics, 2020. 3
- [37] Jonas Pfeiffer, Aishwarya Kamath, Andreas Rücklé, Kyunghyun Cho, and Iryna Gurevych. Adapterfusion: Non-destructive task composition for transfer learning. In *Proceedings of the 16th Conference of the European Chapter of the Association for Computational Linguistics: Main Volume, EACL 2021, Online, April 19 - 23, 2021*, pages 487–503. Association for Computational Linguistics, 2021. 3
- [38] Rajesh PN Rao and Dana H Ballard. Predictive coding in the visual cortex: a functional interpretation of some extraclassical receptive-field effects. *Nature neuroscience*, 2(1): 79–87, 1999. 6
- [39] James Requeima, Jonathan Gordon, John Bronskill, Sebastian Nowozin, and Richard E Turner. Fast and Flexible Multi-Task Classification using Conditional Neural Adaptive Processes. In *Advances in Neural Information Processing Systems*. Curran Associates, Inc., 2019. 3
- [40] Andreas Rücklé, Gregor Geigle, Max Glockner, Tilman Beck, Jonas Pfeiffer, Nils Reimers, and Iryna Gurevych. Adapterdrop: On the efficiency of adapters in transformers. In *Proceedings of the 2021 Conference on Empirical Methods in Natural Language Processing, EMNLP 2021, Virtual Event / Punta Cana, Dominican Republic, 7-11 November, 2021*, pages 7930–7946. Association for Computational Linguistics, 2021. 3
- [41] Olga Russakovsky, Jia Deng, Hao Su, Jonathan Krause, Sanjeev Satheesh, Sean Ma, Zhiheng Huang, Andrej Karpathy, Aditya Khosla, Michael Bernstein, Alexander C. Berg, and Li Fei-Fei. ImageNet Large Scale Visual Recognition Challenge. *International Journal of Computer Vision (IJCV)*, 115(3):211–252, 2015. 1, 4, 7, 8, 12, 13
- [42] Chinmay Savadikar, Michelle Dai, and Tianfu Wu. Learning to grow artificial hippocampi in vision transformers for resilient lifelong learning. *arXiv preprint arXiv:2303.08250*, 2023. 3, 5, 8
- [43] Baifeng Shi, Trevor Darrell, and Xin Wang. Top-down visual attention from analysis by synthesis. In *IEEE/CVF Conference on Computer Vision and Pattern Recognition, CVPR 2023, Vancouver, BC, Canada, June 17-24, 2023*, pages 2102–2112. IEEE, 2023. 6, 12
- [44] Baifeng Shi, Siyu Gai, Trevor Darrell, and Xin Wang. Refocusing is key to transfer learning. *arXiv preprint arXiv:2305.15542*, 2023. 2, 3, 6, 7, 8, 12
- [45] Sebastian Thrun and Tom M Mitchell. Lifelong robot learning. In *The biology and technology of intelligent autonomous agents*, pages 165–196. Springer, 1995. 2

- [46] Ashish Vaswani, Noam Shazeer, Niki Parmar, Jakob Uszkoreit, Llion Jones, Aidan N. Gomez, Lukasz Kaiser, and Illia Polosukhin. Attention is all you need. In *Advances in Neural Information Processing Systems 30: Annual Conference on Neural Information Processing Systems 2017, December 4-9, 2017, Long Beach, CA, USA*, pages 5998–6008, 2017. [2](#), [3](#), [4](#)
- [47] Max Vladymyrov, Andrey Zhmoginov, and Mark Sandler. Continual few-shot learning using hypertransformers. *arXiv preprint arXiv:2301.04584*, 2023. [3](#)
- [48] Johannes von Oswald, Christian Henning, Benjamin F. Grewe, and João Sacramento. Continual learning with hypernetworks. In *International Conference on Learning Representations*, 2020. [3](#)
- [49] Catherine Wah, Steve Branson, Peter Welinder, Pietro Perona, and Serge Belongie. *The Caltech-UCSD Birds-200-2011 Dataset*. 2011. [6](#)
- [50] Haixin Wang, Xinlong Yang, Jianlong Chang, Dian Jin, Jinnan Sun, Shikun Zhang, Xiao Luo, and Qi Tian. Mode approximation makes good vision-language prompts. *arXiv preprint arXiv:2305.08381*, 2023. [3](#)
- [51] Li Yin, Juan M. Perez-Rua, and Kevin J. Liang. Sylph: A hypernetwork framework for incremental few-shot object detection. In *IEEE/CVF Conference on Computer Vision and Pattern Recognition, CVPR 2022, New Orleans, LA, USA, June 18-24, 2022*, pages 9025–9035. IEEE, 2022. [3](#)
- [52] Xiaohua Zhai, Joan Puigcerver, Alexander Kolesnikov, Pierre Ruysen, Carlos Riquelme, Mario Lucic, Josip Djolonga, André Susano Pinto, Maxim Neumann, Alexey Dosovitskiy, Lucas Beyer, Olivier Bachem, Michael Tschannen, Marcin Michalski, Olivier Bousquet, Sylvain Gelly, and Neil Houlsby. The visual task adaptation benchmark. *CoRR*, abs/1910.04867, 2019. [6](#), [7](#), [12](#)
- [53] Qingru Zhang, Minshuo Chen, Alexander Bukharin, Pengcheng He, Yu Cheng, Weizhu Chen, and Tuo Zhao. Adaptive budget allocation for parameter-efficient fine-tuning. In *The Eleventh International Conference on Learning Representations, ICLR 2023, Kigali, Rwanda, May 1-5, 2023*. OpenReview.net, 2023. [3](#)
- [54] Renrui Zhang, Jiaming Han, Aojun Zhou, Xiangfei Hu, Shilin Yan, Pan Lu, Hongsheng Li, Peng Gao, and Yu Qiao. Llama-adapter: Efficient fine-tuning of language models with zero-init attention. *CoRR*, abs/2303.16199, 2023. [3](#)
- [55] Yuanhan Zhang, Kaiyang Zhou, and Ziwei Liu. Neural prompt search. *CoRR*, abs/2206.04673, 2022. [3](#)
- [56] Dominic Zhao, Seijin Kobayashi, João Sacramento, and Johannes von Oswald. Meta-learning via hypernetworks. In *4th Workshop on Meta-Learning at NeurIPS 2020 (MetaLearn 2020)*. NeurIPS, 2020. [3](#)
- [57] Andrey Zhmoginov, Mark Sandler, and Maksym Vladymyrov. HyperTransformer: Model generation for supervised and semi-supervised few-shot learning. In *Proceedings of the 39th International Conference on Machine Learning*, pages 27075–27098. PMLR, 2022. [3](#)
- [58] Bolei Zhou, Aditya Khosla, Agata Lapedriza, Aude Oliva, and Antonio Torralba. Learning deep features for discriminative localization. In *Proceedings of the IEEE conference on computer vision and pattern recognition*, pages 2921–2929, 2016. [6](#)
- [59] Daquan Zhou, Zhiding Yu, Enze Xie, Chaowei Xiao, Animashree Anandkumar, Jiashi Feng, and José M. Álvarez. Understanding the robustness in vision transformers. In *International Conference on Machine Learning, ICML 2022, 17-23 July 2022, Baltimore, Maryland, USA*, pages 27378–27394. PMLR, 2022. [6](#)

A. Appendix

We will first present details of implementation (Sec. B), and then elaborate on the interpretability aspect of our proposed GIFT (Sec. C).

B. Implementation Details

For all the experiments, we use ViT-B/16 model [9], which contains 12 transformer blocks, each with 12 heads in the Multi-Head Self-Attention (MHSA) blocks, and a dimension of 768. For a fair comparison with prior works, we use Stochastic Gradient Descent (SGD) with momentum in the optimization, and train for 100 epochs with a batch size of 32. All our experiments use a momentum of 0.9 and a Cosine decay schedule for the learning rate. For both VTAB and FGVC experiments, we use a hyperparameter search using the validation sets to determine the learning rate and the magnitude for weight decay for each dataset (similar to TOAST [44]). We do not apply weight decay on the clustering parameters since we find that doing so reduces the cluster diversity. This is primarily because weight decay will draw the weights to zero. We also exclude all the bias parameters from weight decay following the common practice. The final hyperparameters are present in `args.yaml` in the log directory of each experiment.

B.1. The VTAB Benchmark

We evaluate our proposed GIFT on the VTAB benchmark [52] using checkpoints from the ViT-B/16 model pretrained on the ImageNet1k [41]¹ and ImageNet21k [7]² under the supervised training protocol. We use the same checkpoints as [44]. For our GIFT, we do a grid search over learning rates $\{0.5, 0.25, 0.1\}$ and weight decays $\{0.01, 0.001, 0.0001, 0.0\}$, and use a transformer dimension of 48 for the hyper-Transformer. For experiments with the LoRA [19] applied to the projection layer, we do a grid search over learning rates $\{2.0, 1.5, 1.0, 0.5, 0.1\}$ and weight decays $\{0.01, 0.001, 0.0001, 0.0\}$. We use the same training, validation, and test splits as [44]. We conduct all the experiments on a single Nvidia Quadro RTX 8000 GPU.

B.2. The FGVC Benchmark

We evaluate our GIFT on the 5 FGVC datasets using the checkpoint from ViT-B/16 pretrained on ImageNet1k [41] (with the same weights¹ from [44]). For our GIFT, we do a grid search over learning rates $\{0.5, 0.25, 0.1\}$ and weight decays $\{0.1, 0.01, 0.001, 0.0001, 0.0\}$, and use the transformer dimension of 192 in the hyper-Transformer. We

¹<https://berkeley.box.com/shared/static/zblb41fqoiyuiyo94a496h45qlqel6r8.pth>

²<https://berkeley.box.com/shared/static/kbsnodpqvowt1lze451kuh90qxwtsxsu.pth>

use a larger dimension than the one used for VTAB experiments to account for the larger size and complexity of the FGVC datasets. Our initial studies indicate that this larger size performs slightly better. For experiments with the LoRA [19] applied to the projection layer, we do a grid search over learning rates $\{2.0, 1.5, 1.0, 0.5, 0.1\}$ and weight decays $\{0.01, 0.001, 0.0001, 0.0\}$. We use the same train, validation and test splits as [44], *except for* Stanford Cars dataset [10]. Due to the unavailability of the dataset from the **original source**, and the difference in the format of the data provided by the **updated source**, we create our own training and validation split (with the same number of images as [44]) and use the official testing split. We conduct all the experiments on a single Nvidia Tesla V100 GPU.

C. More Qualitative Results on the Interpretability of GIFT

C.1. Concept Clusters

Fig. 5 shows that our proposed GIFT can encode similar concepts across different classes in the same layers (but through different clusters). See the caption for details.

C.2. Class-Specific Clusters

Figure 6 shows that GIFT can form clusters that reflect properties of a specific class along with concept clusters. See the caption for details.

C.3. Behavior under multiple classes

The analysis till now shows that the parameter-to-cluster (PaCa) attention module in our proposed GIFT can form clusters on the objects of interest in the images. A natural next question is to ask how the clusters will behave when multiple objects of different classes are present in the image. To test this, we construct a mosaic image containing the same 4 images studied in Section C.1 and Section C.2. We create the mosaic image by first adding the positional embeddings to image tokens created using the convolutional patch embedding in the Vision Transformer (ViT) architecture, and then concatenating the tokens along the token dimension. This preserves the content and positional information in the image, but the token-to-token interactions in the attention mechanism of the ViT is not constrained to just one image. Figure 7 shows that the PaCa module in GIFT can form clusters on multiple instances of objects simultaneously (although the class prediction suffers). This shows the potential of our proposed method for object localization under minimal supervision. Note that [43] also shows similar behavior, and can control the attention of the network using a token selection mechanism. Future works can explore how our method can be extended for a precise control of attention for targeted localization.

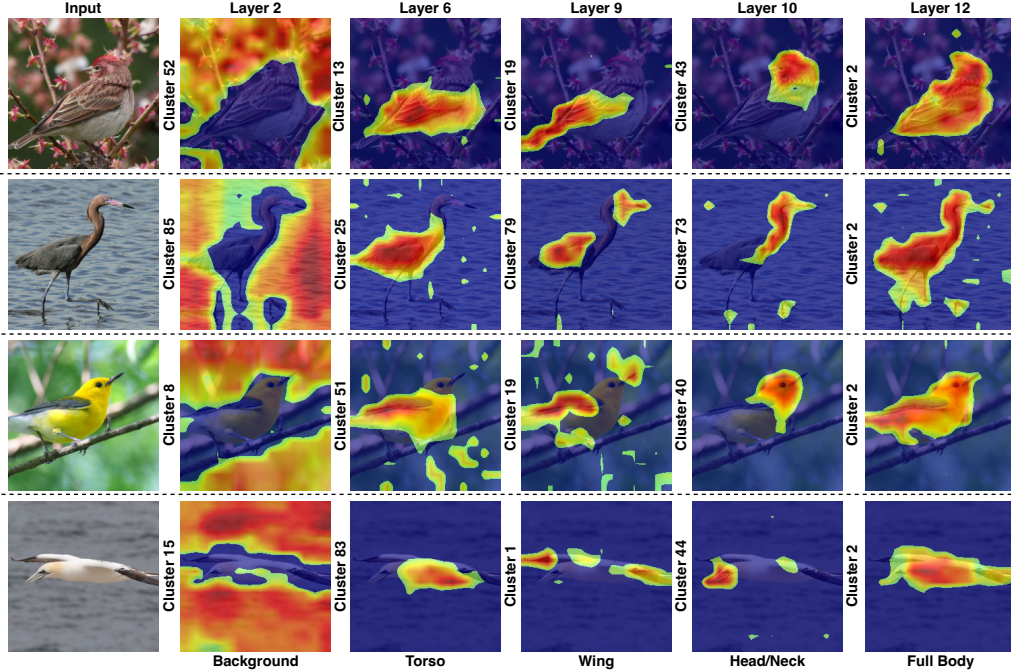


Figure 5. **Concept Clusters:** We observe that GIFT can encode similar concepts across different classes in the same layers (but through different clusters). For example, for birds in the testing set of the NABirds dataset [16], clusters encoding the background can be found in layer 2 (the 1st column), clusters encoding the torso can be found in layer 6 (the 2nd column), clusters for the wings (along with some class specific attributes) can be found in layer 9 (the 3rd column), clusters for the head (and neck) can be found in layer 10 (the 4th column). Interestingly, the same cluster encodes the entire body of the bird in layer 12 (the last column), the layer right before the classification head.

C.4. Cluster development throughout training

Figure 8 shows at what point in the training various clusters are formed. It can be seen that clusters that focus on specific details of the image are formed late in the training, whereas clusters that focus on the entire object (in this case, the entire bird) are formed very early. See caption for details.

C.5. Qualitative results on Oxford Flowers, Stanford Cars, Stanford Dogs, ImageNet

Figures 9, 10, 11, and 12 show additional clusters on Oxford Flowers [35], Stanford Cars [10], Stanford Dogs [24] and ImageNet1k [41]. See captions of the respective figures for details.

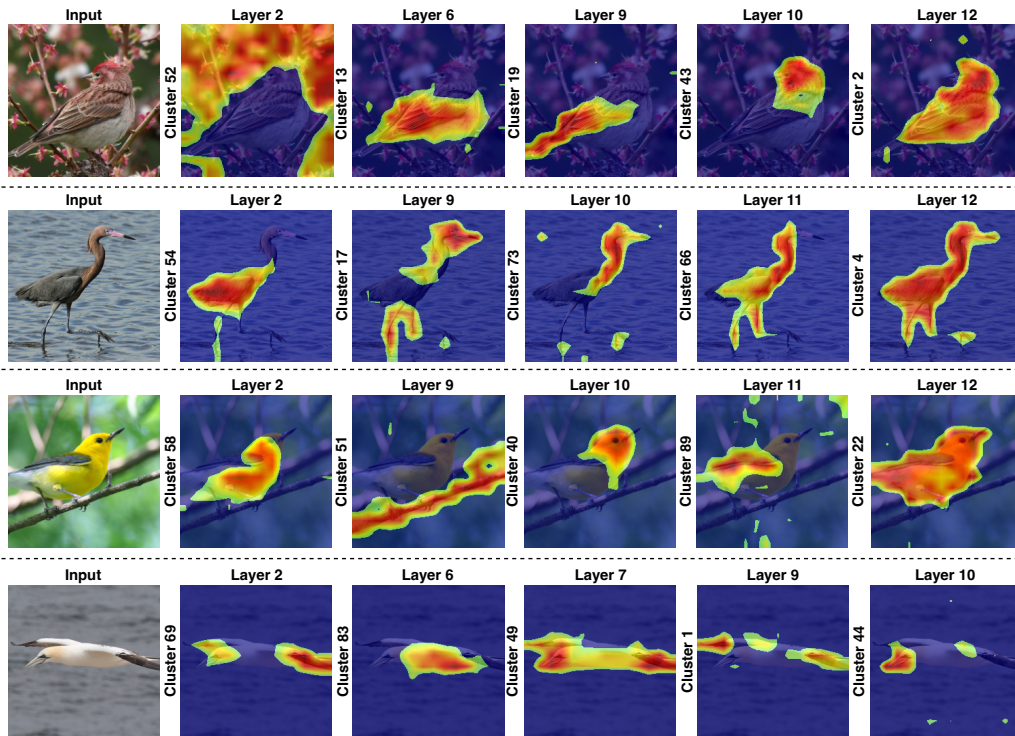


Figure 6. **Class Specific Clusters:** Along with concept clusters, clusters that reflect the properties of a specific class also occur in our proposed GIFT. For example in the class Reddish Egret (Dark Morph) (2nd row), clusters corresponding to the distinctive neck, beak and legs can be seen. Notably, for Prothonotary Warbler (3rd row), a cluster representing a twig of a tree can also be seen. We hypothesize that this is because almost all the images of this class from the dataset are images of the bird sitting on a twig. Although an undesirable behavior, this shows the interpretable nature of GIFT. We leave addressing how to avoid this behavior to future work.

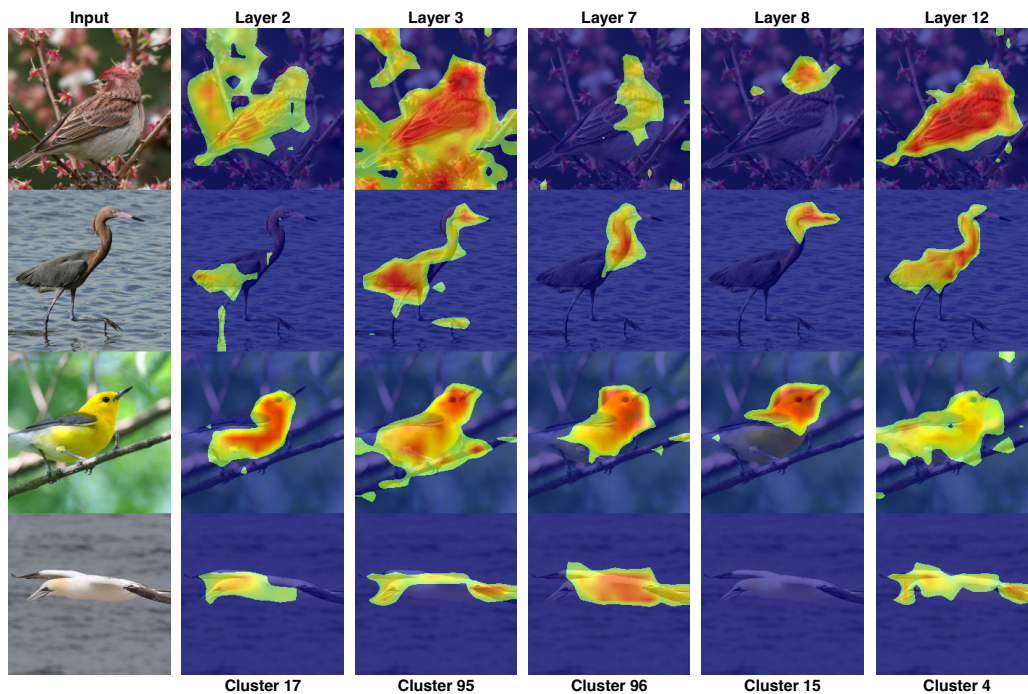
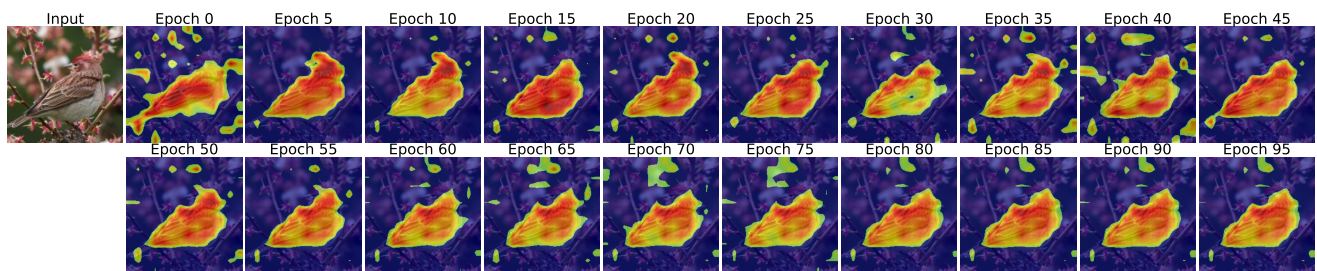
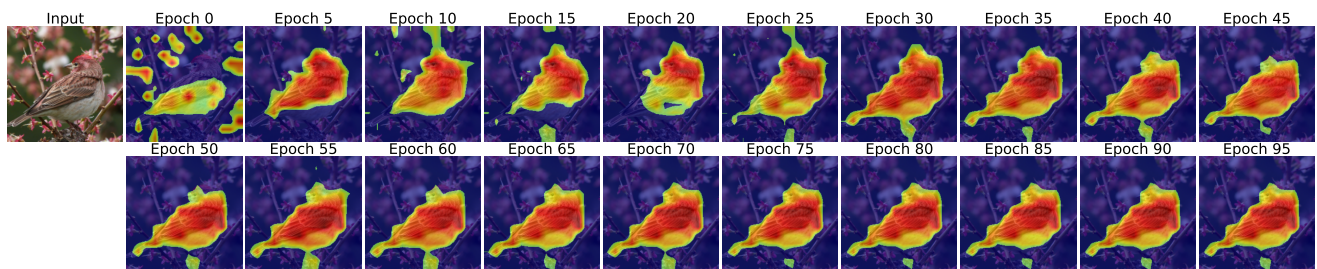


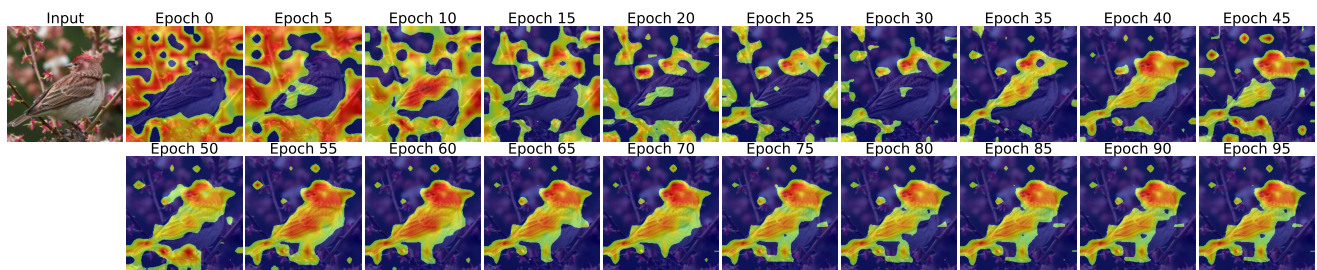
Figure 7. **Mosaic Image:** PaCa module in GIFT can form clusters over multiple objects of different classes at the same time, even though it is trained on images containing a single object of interest. For example, Cluster 15 in Layer 8 can localize the heads of birds, and Cluster 4 in Layer 12 can localize the entire body of multiple birds at the same time. We note that the clusters are more noisy than the ones formed for single images. However, this shows the potential of our method for object localization under minimal supervision, which we leave for future work.



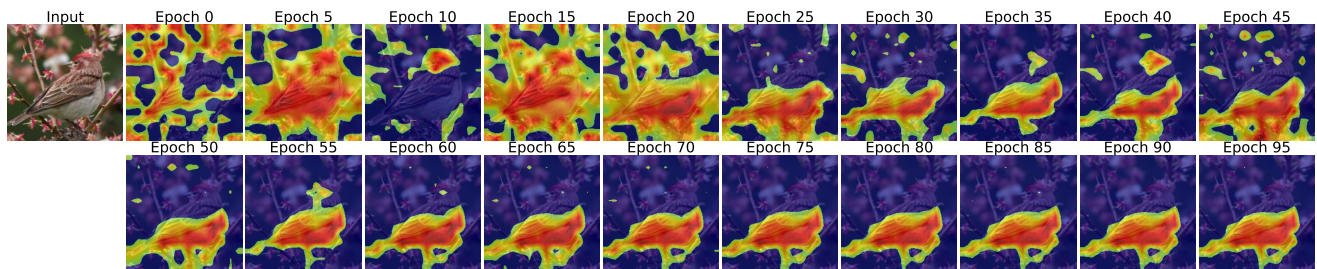
(a) **Cluster 2, Layer 12:** Entire body of the bird.



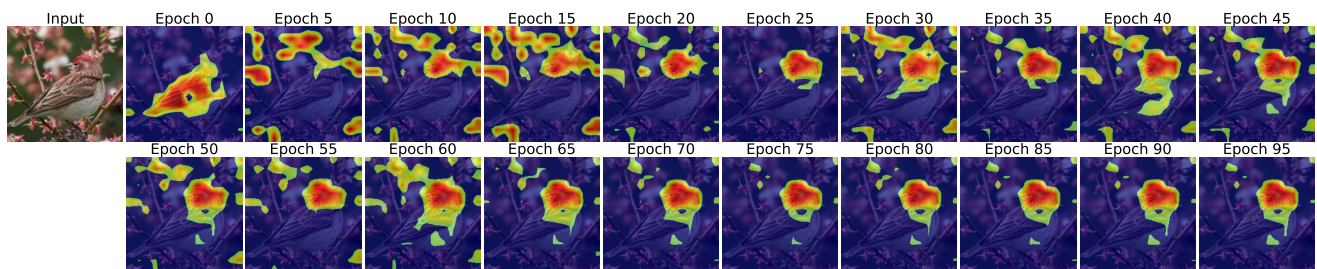
(b) **Cluster 25, Layer 8:** Entire body of the bird.



(c) **Cluster 12, Layer 12:** Head, wing and tail of the bird.



(d) **Cluster 5, Layer 9:** Torso of the bird.



(e) **Cluster 43, Layer 10:** Head of the bird.

Figure 8. Cluster formation with number of training epochs. Clusters that focus on the entire object (Cluster 2 in Layer 12, and Cluster 25 in Layer 8) are formed very early in the training. Clusters that focus on specific details of the image (Cluster 12 in Layer 12, Cluster 5 in Layer 9, and Cluster 43 in layer 10) are formed late in the training.

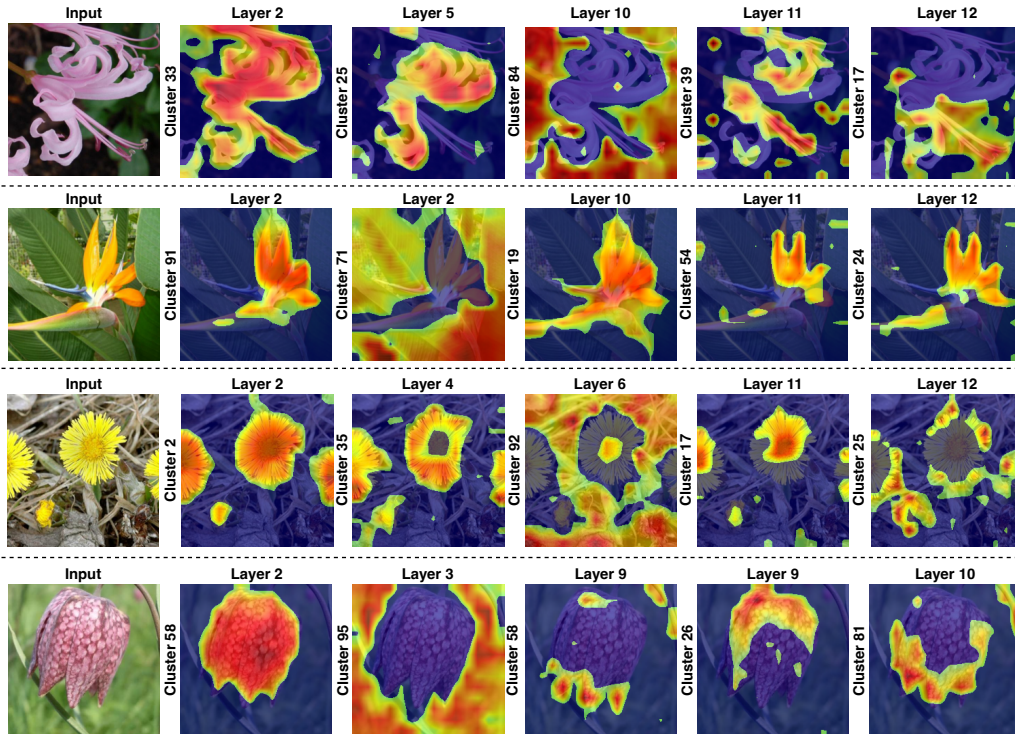


Figure 9. **Oxford Flowers:** The PaCa module in GIFT can form relevant clusters over the petals (and other parts) of the flowers. Clusters can focus on very specific parts of the flower like the tips of the petals (Row 3 Column 6, Row 4 Columns 4 and 6), or the whole flower. The clusters are class-specific.

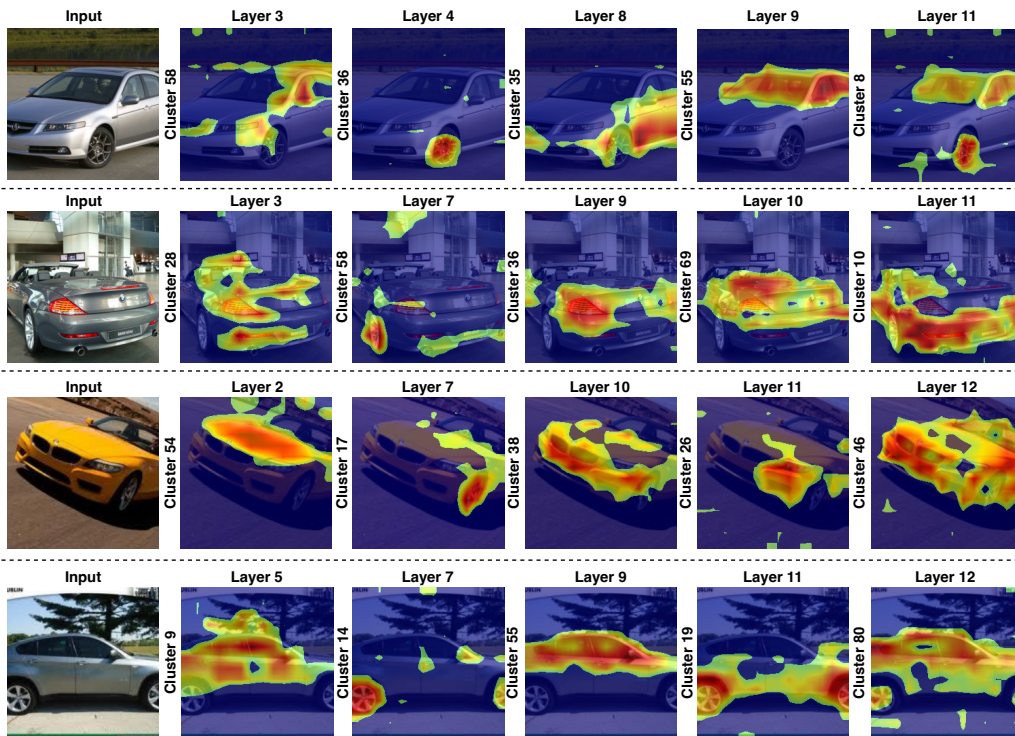


Figure 10. **Stanford Cars:** The PaCa module in GIFT can form various clusters focusing on different parts of the car. For example, clusters encoding the wheels (Column 3), windshield (Row 1, column 5), bonnet (Row 3, Column 2), headlight (Row 3, Column 5), etc. can be found.

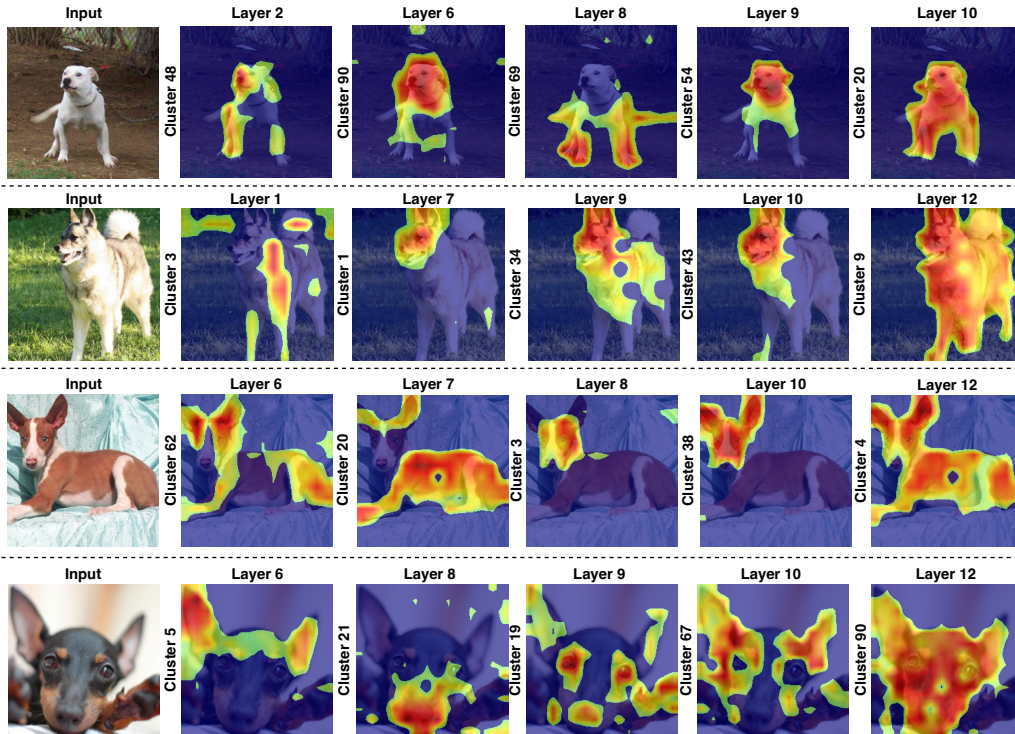


Figure 11. **Stanford Dogs:** The PaCa module in GIFT forms clusters over various parts of the dog’s anatomy, many of which are unique for a class. For example, in Rows 3 and 4, clusters on the ears, eyes, snout and face can be found. In Row 4, clusters on the head, torso and a combination of both are formed.

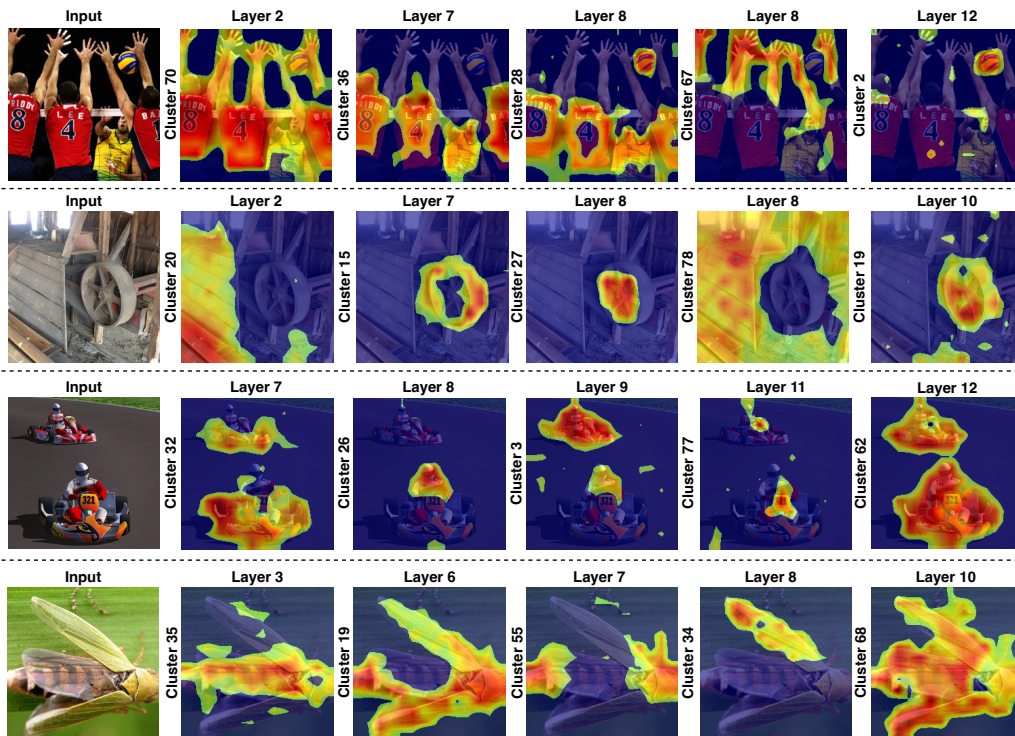


Figure 12. **ImageNet:** Even on a large and diverse dataset like ImageNet, the PaCa module can form clusters over relevant parts of the image. The 4 images (taken from the official validation set) all show different image characteristics, but the clusters still focus on the relevant aspects of the image.